*EVS28*
*KINTEX, Korea, May 3-6, 2015*

# Comparison of IPM and SPM motors using ferrite magnets for low-voltage traction systems

Yong-Hoon Kim[1], Suwoong Lee[1], Eui-Chun Lee[1], Bo Ram Cho[1] and Soon-O Kwon[1]
[1]*Technology Convergence R&BD Group, Korea Institute of Industrial Technology, Daegu, Korea, kso1975@kitech.re.kr*

**Abstract**

Permanent magnet synchronous motors are widely employed for electric vehicles (EVs) because of their high torque density and efficiency. However, rare-earth magnets have critical disadvantages such as an unstable supply and high cost. In order to solve these problems, ferrite magnets are being considered for these motors as an alternative to rare-earth permanent magnets (PMs). This paper compares interior permanent magnet (IPM) and surface-mounted permanent magnet (SPM) motors using ferrite magnets for a low-voltage system EV under the same design conditions. The IPM and SPM motors were compared under the same voltage and current through *d-q* axis equivalent analysis. The results confirmed the applicability of ferrite motors to low-voltage system EVs.

*Keywords: ferrite magnet, low voltage system, electric vehicle*

## 1 Introduction

As environmental problems increase, research and development into high-efficiency motors is underway to replace power sources based on conventional fossil fuels in various industries. Part of this effort has involved the development of an in-wheel type motor as a power source for electric vehicles. An in-wheel type motor can maximize the output transmission effect by directly driving the wheels of the vehicle. Furthermore, it reduces weight by simplifying the devices of the drive system [1, 2].

However, the supply instability and rising prices of rare-earth permanent magnets (PMs), which are essential elements in high-power motors, are posing challenges to the development of many motors, including in-wheel type motors.

In recent years, ferrite-type PMs, which do not have price and supply problems, are being studied as replacements for rare-earth PMs in existing motors.

Because most studies on replacing existing rare-earth motors with ferrite motors have been on high-voltage systems, the motors have been designed as spoke or interior permanent magnet (IPM) types, which use the reluctance and magnetic torque through current phase control, rather than as surface-mounted permanent magnet (SPM) types, which only use magnetic torque [3-6]. However, the performances of the IPM and SPM types have not been compared for low-voltage systems where the current phase control of high-speed sections is difficult because of voltage limitations.

In this study, IPM- and SPM-type in-wheel motors using ferrite PMs were designed under low-voltage system conditions to drive a golf cart. Finite element analysis (FEA) and *d-q* axis equivalent circuit analysis were used for the design process. The design results were compared and analysed to determine which of the IPM and SPM types is appropriate for low-voltage systems.

## 2 Design of IPMSM and SPMSM with ferrite PM for low voltage system

In this study, motors were developed with the objective of reducing the cost compared to motors that use conventional rare-earth magnets. The NdFeB PM was replaced with a ferrite magnet to reduce the cost.

In-wheel-type IPM and SPM synchronous motors (SMs) using ferrite were designed to have the same volume as existing Nd magnet in-wheel motors. The motor of each type was designed to have a shape that meets all operation and design requirements through FEA and *d-q* axis equivalent circuit analysis [7].

### 2.1 *D-q* axis equivalent circuit analysis theory

*D-q* axis equivalent circuit analysis is generally used for motor characterization. FEA can be used to derive accurate results; however, it is inefficient for characterization over a wide operating range.

Figure 1 shows the equivalent circuit of a general PMSM [8].

The PM is an equivalent circuit composed of a *d-q* axis synchronous coordinate system that includes the iron loss resistance, as shown in Figure 1. The mathematical model of the *d-q* axis equivalent circuit including the iron loss resistance $R_c$ is expressed by Eqs. (1)–(3). Here, $i_d$ and $i_q$ are the *d*- and *q*-axis currents, respectively. $i_{cd}$ and $i_{cq}$ are the *d*- and *q*-axis iron loss currents, respectively. $v_d$ and $v_q$ are the d- and *q*-axis terminal voltages, respectively, and $R_a$ is the resistance of the armature winding. $\Psi_a$ is the magnetic flux inter-linkage amount per pole, and $L_d$ and $L_q$ indicate the *d*- and *q*-axis inductances. Finally, $P_n$ is the pole pair count [9].

$$\begin{bmatrix} v_d \\ v_q \end{bmatrix} = R_a \begin{bmatrix} i_{od} \\ i_{oq} \end{bmatrix} + \left(1 + \frac{R_a}{R_c}\right) \begin{bmatrix} v_{od} \\ v_{oq} \end{bmatrix} + p \begin{bmatrix} L_d & 0 \\ 0 & L_q \end{bmatrix} \begin{bmatrix} i_{od} \\ i_{oq} \end{bmatrix} \quad (1)$$

$$\begin{bmatrix} v_{od} \\ v_{oq} \end{bmatrix} = \begin{bmatrix} 0 & -\omega L_q \\ \omega L_d & 0 \end{bmatrix} \begin{bmatrix} i_{od} \\ i_{oq} \end{bmatrix} + \begin{bmatrix} 0 \\ \omega \psi_a \end{bmatrix} \quad (2)$$

$$T = P_n \left\{ \psi_a i_{oq} + \left(L_d - L_q\right) i_{od} i_{oq} \right\} \quad (3)$$

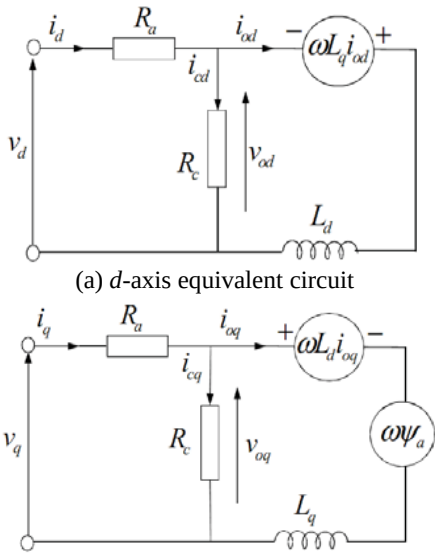


(a) *d*-axis equivalent circuit

(b) *q*-axis equivalent circuits

Figure 1 : Equivalent circuits of PMSM

### 2.2 Specification of in-wheel motor

Table 1 lists the system conditions of the designed motor. The motor has a DC link voltage of 72 V and size constraints of 250 mm for the stator outer diameter and 32 mm for the stack length. A concentrated winding combination of 16 poles and 24 slots was selected in consideration of the inverter and production costs. The design conditions were limited so that the motor would attain a maximum output of 3 kW and maximum torque of 30 Nm. The base and maximum speeds of the motor are 915 and 3100 rpm, respectively. Finally, the PM was required to have a residual magnetic flux density of 0.4 T at 65 ℃.

Table 1 : Requirements for In-wheel type motors with ferrite PM design

| Item | Value |
|---|---|
| DC link voltage (V) | 72 |
| Stator outer diameter (mm) | 250 |
| Stack length (mm) | 32 |
| Pole/slot number | 16 / 24 |
| Max. power (kW) | 3 |
| Max. torque (Nm) | 30 |
| Base/Max. speed (rpm) | 915/3100 |
| PM Br(@65°C) (T) | 0.4 |
| Core material | 50PN470 |

### 2.3 Design of In-wheel IPMSM and SPMSM with ferrite magnets

An IPMSM and SPMSM using ferrite were designed to meet the conditions in Table 1 through

FEM and *d-q* axis equivalent circuit analysis. Figure 2(a) and (b) show the shapes of the stator and rotor of the IPMSM, and Figure 3(a) and (b) show the shapes of the stator and rotor of the SPMSM.

The shape of each motor was designed according to the rotor shape, which included the PM, shape of the stator, and number of coil turns, which needed to satisfy the back electromotive force (EMF) and inductance requirements for the pole slot combination and performance.

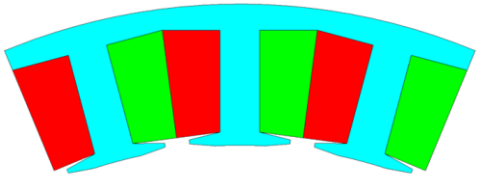

(a) Stator shape

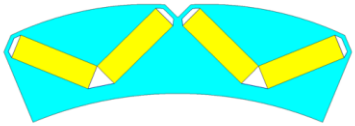

(b) Rotor shape

Figure 2: Shape of IPMSM with ferrite PM

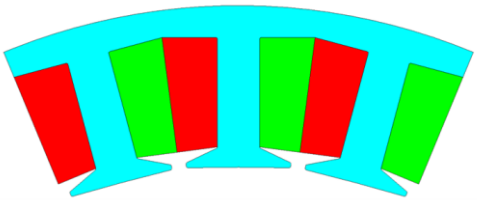

(a) Stator shape

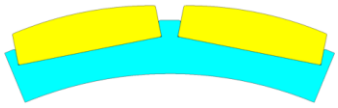

(b) Rotor shape

Figure 3 : Shape of SPMSM with ferrite PM

Table 2 : Design summary of in-wheel type motors with ferrite PM design

| Item | IPMSM | SPMSM |
|---|---|---|
| Series turns per phase | 56 | 64 |
| Number of parallel circuits | 8 | |
| Fill factor (%) | 37.9 | 37.8 |
| Rotor diameter (mm) | 191.5 | 182.5 |
| Current density ($A/mm^2$) | 10 | 10.3 |
| Permanent magnet volume ($mm^3$) | 5360 | 7126.4 |

### 2.3.1 Back EMF results of in-wheel PMSM with ferrite

Figure 4(a) and (b) show the harmonic analysis results, phase back-EMF of the designed motors. Both the IPMSM and SPMSM had low back-EMF harmonics because they were applied with the chamfer of the stator and the eccentricity of the rotor to remove the harmonic impact of the torque ripple and back-EMF.

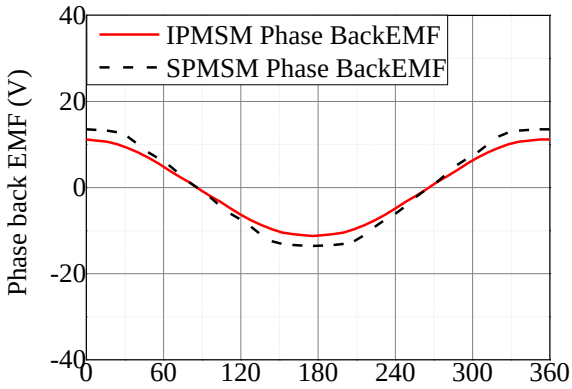


(a) Phase Back

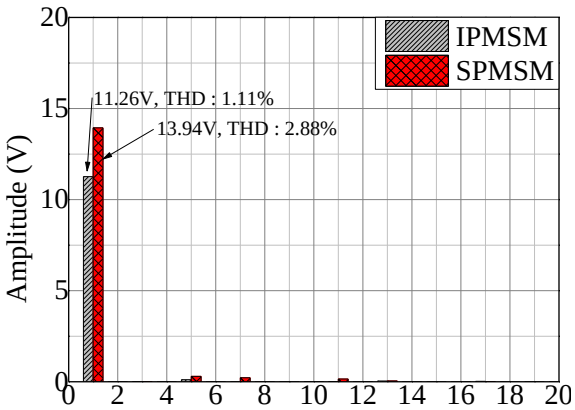


(b) Harmonic component

Figure 4: Back EMF of IPMSM and SPMSM with ferrite PM

### 2.3.2 Inductance results of in-wheel PMSM with ferrite

Figure 5(a) and (b) show the inductance according to the current magnitude and phase angle of the designed motors.

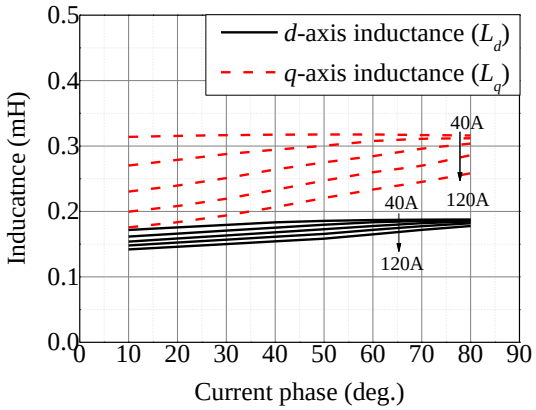


(a) IPMSM

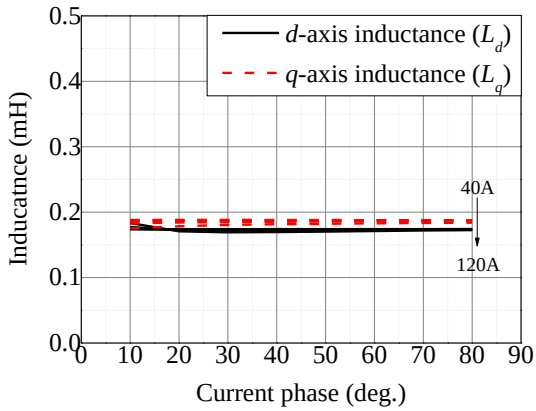


(b) SPMSM

Figure 5: *d-q* axis Inductance

Because the number of stator coil turns for the IPMSM (48 turns) was 25% less than that for the SPMSM (64 turns), the IPMSM must have a lower inductance than the SPMSM proportional to the square of the difference in the number of turns if all other conditions are the same. However the size of the actual air gap is significant because the PM of the designed SPMSM was thick. Also, the V-type placement of the PMs in the IPMSM increases the core area between the air gap and PM and increases the *q*-axis inductance. Hence, the inductance of the IPMSM, especially the *q*-axis inductance, was more significant than that of the SPMSM despite the former having fewer coil turns than the latter.

### 2.3.3 *D-q* axis equivalent circuit analysis results of in-wheel PMSM with ferrite

*D-q* axis equivalent circuit analysis was performed to verify whether the relevant motor meets the performance requirements for operation. Table 3 lists the analysis conditions, and then Figure 6(a)-(d) shows the *d-q* axis equivalent circuit analysis results of the two motors.

Figure 6(a) showed that the two electric motors meet the torque and output conditions. However, IPMSM used high current phase angle and more input current at the base speed in having a smaller phase back-EMF than SPMSM. Therefore IPMSM was line-to-line voltage saturation is earlier than SPMSM.

Table 3: *d-q* axis equivalent circuit analysis condition

| Item | IPMSM | SPMSM |
|---|---|---|
| Pole | 16 | |
| Max. Line-line voltage ($V_{rms}$) | 48 ($V_{dc}$: 72V) (Modulation: 95%) | |
| Phase back EMF ($V_{rms}$) | 7.96 | 9.86 |
| Phase resistance (mΩ) | 19.14 | 19.54 |

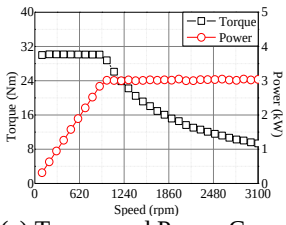


(a) Torque and Power Current

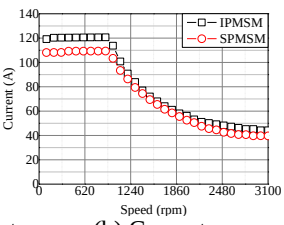


(b) Current

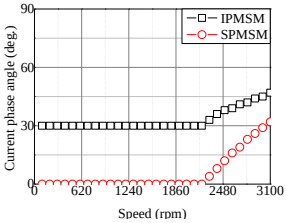


(c) Current phase angle

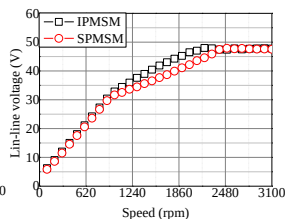


(d) Line to line voltage

Figure 6: *D-q* axis equivalent circuit analysis results

# 3 Comparison of load condition between IPMSM and SPMSM with ferrite PM

The characteristics of the IPMSM and SPMSM under loading conditions were compared to determine which is appropriate for low-voltage systems.

For the driving of a motor in a low-voltage system, the peak value of the back-EMF waveform under a load should never exceed the voltage limit. Because this constraint can be a major problem, the peak value of the line-to-line back-EMF waveform under a load must be determined.

Figure 7 shows the line-to-line back-EMF waveforms of the IPMSM and SPMSM under loads.

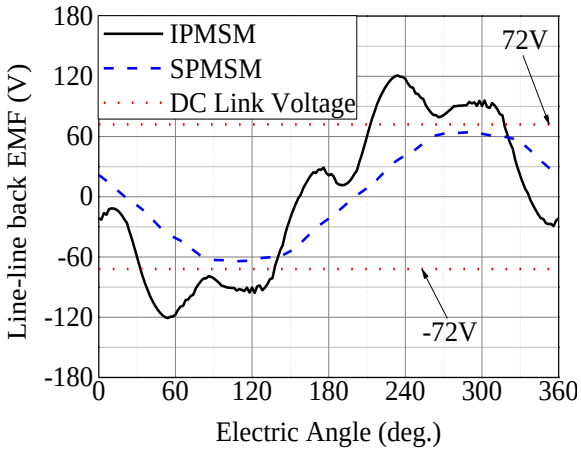


Figure 7: Line to line back EMF at load condition (@Max speed)

The line-to-line back-EMF waveform of the SPMSM under a load showed a lower peak value than that of the IPMSM. Therefore, the former is less likely to exceed voltage limitations during driving. The IPMSM recorded a line-to-line back-EMF that exceeded the DC link voltage and hence could not meet the voltage limitation conditions. The torque waveform was compared under the maximum speed conditions to accurately review the above. Figure 8 shows the torque waveforms of the IPMSM and SPMSM. Even after the chamfer of the stator and eccentricity of the rotor were applied to reduce the torque ripple in the IPMSM, this motor still showed a significant torque ripple under the current conditions at the maximum speed and had a wave form that made driving difficult. Figure 9 (a) and (b) showed that the waveform was severely distorted, and the flux linkage between the rotor and stator was not properly achieved. This explains the improper transmission of the flux generated in the rotor of the IPMSM based on changes in the current phase angle to the stator and the leakage situation. Based on analysis, such phenomena appear when the air barrier of the rotor is not sufficiently saturated according to the current phase difference when a ferrite PM is used. In contrast, the air barrier of the rotor is sufficiently saturated in the case of an Nd magnet.

On the other hand, Figure 10 (a) and (b) showed that the flux linkage between the rotor and stator was properly achieved. Furthermore this motor showed a suitable torque ripple under the current conditions at the maximum speed.

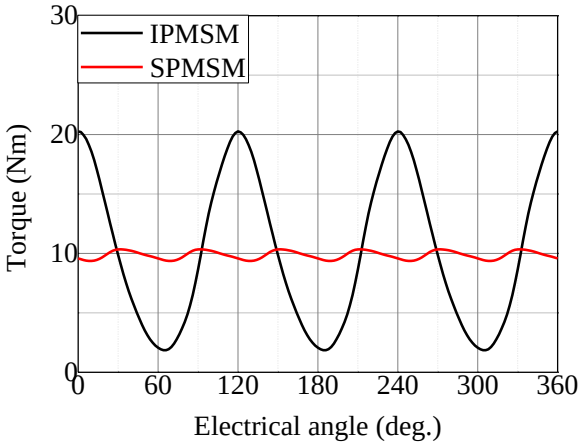


Figure 8: Torque waveform at load condition (@Max speed)

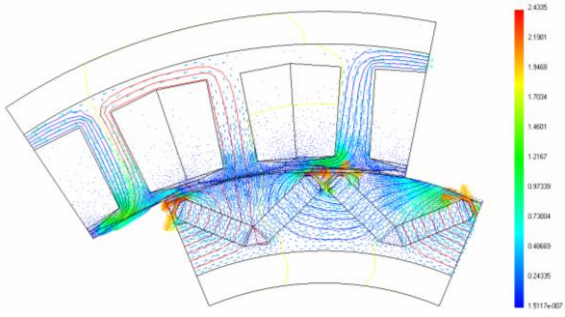

(a) Flux vector

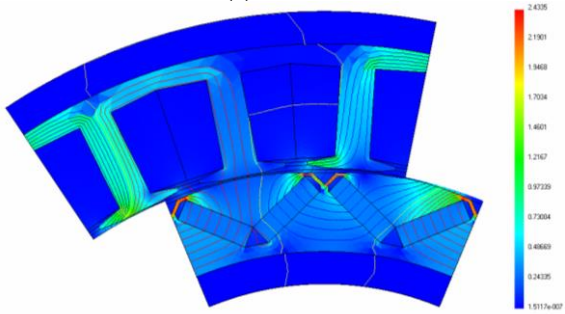

(b) Flux density

Figure 9: Flux vector and flux density of IPMSM

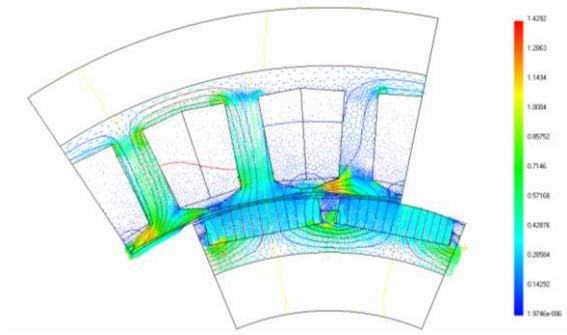

(a) Flux vector

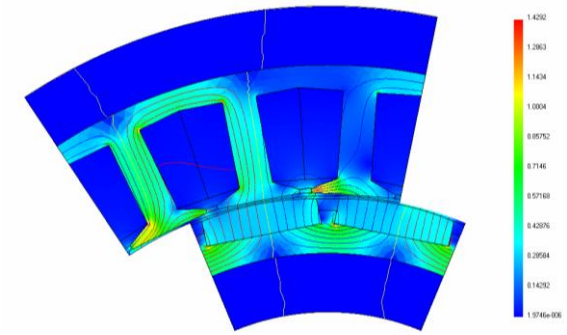

(b) Flux density

Figure 10: Flux vector and flux density of SPMSM

# 4 Conclusion

In this study, a comparative analysis was conducted to assess whether the SPM or IPM is the appropriate type for in-wheel type SMs using ferrite PMs in a low-voltage system. An IPMSM uses both magnetic torque and reluctance torque, so it can obtain the same power density as a SPMSM even with fewer magnets used. However, IPMSM has a higher inductance than a SPMSM because of the decrease *q*-axis magnetic path when PMs are placed within a limited volume. The flux linkage between the rotor and stator decreases, and the distortion of the back-EMF waveform grows owing to the leakage flux in the air barrier of the rotor under a load. For this reason, the IPMSM has a higher peak value for the line-to-line back-EMF waveform than the voltage limit value in low-voltage systems, so the voltage required for driving the motor can be insufficient.

Because the SPMSM cannot use the reluctance torque, it requires more magnets than the IPMSM to produce a similar output. However, when the inductance is relatively small and the current phase is controlled, the distortion in the line-to-line back-EMF waveform are small, which lead to a relatively small peak value. For this reason, the SPMSM more easily meets the voltage conditions of the system.

Based on the PM volume and output density of the motor, an IPMSM can obtain the same output with relatively few magnets, which can be advantageous. However, unlike motors using rare-earth magnets such as NdFeB, an IPMSM under current phase control conditions shows an increase in the magnetic flux leakage of the air barrier and the inductance. As a result, the voltage drop caused by the inductor grows and can exceed the voltage limit. Therefore, the SPMSM, which has low distortions of the line-to-line back-EMF waveform under a load and the inductance, is advantageous for a system with low voltage limits.

# References


[1] K. Sone, M. Takemoto, S. Ogasawara, K. Takezaki, H. Akiyama, A ferrite PM in-wheel motor without rare earth materials for electricity commuters, IEEE Trans. Magn., vol. 48, no. 11, pp. 2961–2964, 2012.

[2] S.-H. Chai, B.-H. Lee, J.-P. Hong, Weight reduction design of in-wheel type motor for power density improvement, EVS26, 2012.

[3] K.-S. Kim, J.-W. Jung, J.-P. Hong, K.-N. Kim, Characteristic analysis of concentrated flux type motor using ferrite magnet, 2012 Summer Conference of Korean Institute of Electrical Engineers (KIEE), pp. 516-517, 2012.

[4] S.-H. Do, B.-H. Lee, H.-Y. Lee, J.-P. Hong, Torque ripple reduction of wound rotor synchronous motor using rotor slits, 2012 15th International Conference on Electrical Machines and Systems (ICEMS), IEEE, 2012.

[5] K. Boughrara, R. Ibtiouen, N. Takorabet, Analytic calculation of magnetic field and electromagnetic performances of spoke type IPM topologies with auxiliary magnets. 2014 International Conference on Electrical Machines (ICEM), IEEE, 2014.

[6] H.-J. Kim, D.-Y. Kim, J.-P. Hong, Structure of concentrated-flux-type interior permanent-magnet synchronous motors using ferrite permanent magnets, IEEE Trans. Magn., vol. 50, no. 11, 2014.

[7] S.-O Kwon, S.-I. Kim, S.-H. Lee, J.-P. Hong, Design of BLDC motor using parametric design, KIEE, pp. 1013-1014, 2007.

[8] B.-H. Lee, S.-O Kwon, J.-P. Hong, H. Nam, Effect of field weakening control of interior permanent

magnet synchronous motor on core loss distribution, 2010 Summer Conference of Korean Institute of Electrical Engineers (KIEE).

[9] J.-W. Jung, J.-J. Lee, S.-O Kwon, J.-P. Hong, K.-N. Kim, Equivalent circuit analysis of interior permanent magnet synchronous motor considering armature reaction, Summer Conference of Korean Institute of Electrical Engineers (KIEE), 2008.

[10] G. Pellegrino, A. Vagati, P. Guglielmi, B. Boazzo. Performance comparison between surface mounted and interior PM motor drives for electric vehicle application, IEEE Trans. Ind. Elec., vol. 59, no. 2, pp. 803-811, ISSN 0278-0046, 2012.

# Authors

Yong-Hoon Kim received a M.S. degree in automotive engineering from Hanyang University, Korea, in 2012. Since 2012, he has been working as a researcher at KITECH, Korea. His main fields of interest are electromagnetic field analysis and electrical motor design related to IPMSMs for vehicle traction.

Suwoong Lee received Ph.D. degree in systems and information engineering from Tsukuba University, Japan, in 2005. Since 2012, he has been working as a senior researcher in the KITECH, Korea. His main fields of interest are human-coexistence/ cooperative type robot and bio-robotics.

Eui-Chun Lee is on the course of master's degree in mechanical engineering from Kyung-Pook National University, Korea, in 2014~. Since 2014, he has been working as a student researcher in the KITECH, Korea. His main fields of interest are electric machine and robot system.

Bo Ram Cho is on the course of Ph.D. degree in physics from Kyung-Pook National University, Korea, in 2013~. Since 2013, he has been working as a researcher in the KITECH, Korea. His main fields of interest are solids physics experiment.

Soon-O Kwon received Ph.D. degree in automotive engineering from the Hanyang University, Korea, in 2010. Since 2011, he has been working as a senior researcher in the KITECH, Korea. His main fields of interests are electromagnetic field analysis and electrical motor design related to the IPMSM for Vehicle traction.